Terahertz surface plasmon polaritons on periodically corrugated metal surfaces

Linfang Shen

Department of Information Science and Electronic Engineering, Electromagnetic Academy, Zhejiang University, Zhejiang Province, Hangzhou 310027, PRC

Xudong Chen

Department of Electrical and computer engineering, National University of Singapore, Singapore 117576

elechenx@nus.edu.sg

Tzong-Jer Yang

Department of Electrophysics, National Chiao Tung University, Hsinchu 30050, Taiwan, ROC

Abstract: Based on a modal expansion of electromagnetic fields, a rigorous method for analyzing surface plasmon polaritons (SPPs) on a periodically corrugated metal surface has been formulated in this paper. This method takes into account the finite conductivity of the metal as well as higher-order modes within the grooves of the surface structure, thus is able to accurately calculate the loss of these spoof SPPs propagating along the structured surface. In the terahertz (THz) frequency range, the properties of the dispersion and loss of spoof SPPs on corrugated Al surfaces are analyzed. For spoof SPPs at THz frequencies, the strong confinement of the fields is often accompanied with considerable absorption loss, but the performance of both low-loss propagation and subwavelength field confinement for spoof SPPs can be achieved by the optimum design of surface structure.

OCIS codes: (240.6680) Surface plasmons; (240.6690) Surface waves; (999.9999) Terahertz.

References and links

1. H. Raether, *Surface Plasmons* (Springer-Verlag, Berlin, 1988).
2. H. E. Ponath and G. I. Stegeman (Eds.), *Nonlinear Surface Electromagnetic Phenomena* (North-Holland, Amsterdam, 1991).
3. V. M. Agranovich and D. L. Mills (Eds.), *Surface Polaritons* (North-Holland, Amsterdam, 1982).
4. A. V. Zayats and I. I. Smolyaninov, "Near-field photonics: surface plasmon polaritons and localized surface plasmons," J. Opt. A: Pure Appl. Opt. **5**, S16-S50 (2003).
5. W. L. Barnes, A. Dereux, and T. W. Ebbesen, "Surface plasmon subwavelength optics," Nature **424**, 824-830 (2003).
6. A. V. Zayats, I. I. Smolyaninov, and A. A. Maradudin, "Nano-optics of surface plasmon polaritons," Physics Reports **408**, 131-314 (2005).
7. S. I. Bozhevolnyi, J. Erland, K. Leosson, P. M. W. Skovgaard, and J. M. Hvam, "Waveguiding in surface plasmon polariton band gap structures," Phys. Rev. Lett. **86**, 3008-3011 (2001).
8. J. F. OHara, R. D. Averitt, and A. J. Taylor, "Terahertz surface plasmon polariton coupling on metallic gratings," Opt. Express **12**, 6397-6402 (2004).
9. J. Saxler, J. Gomez Rivas, C. Janke, H. P. M. Pellemans, P. Haring Bolivar, and H. Kurz, "Time-domain measurements of surface plasmon polaritons in the terahertz frequency range," Phys. Rev. B **69**, 155427-1-4 (2004).
10. J. B. Pendry, L. Martin-Moreno, and F. J. Garcia-Vidal, "Mimicking surface plasmons with structured surfaces," Science **305**, 847-848 (2004).

#86098 - $15.00 USD Received 6 Aug 2007; revised 24 Sep 2007; accepted 24 Sep 2007; published 27 Feb 2008

11. F. J. Garcia-Vidal, L. Martin-Moreno, and J. B. Pendry, "Surfaces with holes in them: new plasmonic metamaterials," J. Opt. A: Pure Appl. Opt. **7**, S97-S101 (2005).
12. S. A. Maier, S. R. Andrews, L. Martin-Moreno, and F. J. Garcia-Vidal, "Terahertz surface plasmon-polariton propagation and focusing on periodically corrugated metal wires," Phys. Rev. Lett. **97**, 176805-1-4 (2006).
13. Y. Chen, Z. Song, Y. Li, M. Hu, Q. Xing, Z. Zhang, L. Chai, and C. Y. Wang, "Effective surface plasmon polaritons on the metal wire with arrays of subwavelength grooves," Opt. Express **14**, 13021-13029 (2006).
14. A. P. Hibbins, B. R. Evans, and J. R. Sambles, "Experimental verification of designer surface plasmons," Science **308**, 670-672 (2005).
15. A. W. Snyder and J. D. Love, *Optical Waveguide Theory* (Chapman & Hall, London, 1983).
16. D. R. Lide, *CRC Handbook of Chemistry and Physics* (CRC Press, Boca Raton, 2004).
17. N. W. Ashcroft and N. D. Mermin, *Solid State Physics* (Saunders College, Philadelphia, 1976).
18. M. Nagel, A. Marchewka, and H. Kurz, "Low-index discontinuity terahertz waveguides," Opt. Express **14**, 9944-9954 (2006).
19. S. Q. Lou, T. Y. Guo, H. Fang, H. L. Li, and S. S. Jian, "A new type of terahertz waveguides," Chin. Phys. Lett. **23**, 235-238 (2006).

1. Introduction

Surface plasmon polaritons (SPPs) are surface electromagnetic (EM) waves, whose fields can be highly confined to dielectric-metal interfaces [1]. This confinement leads to a significant enhancement of the EM field at the interface, which is responsible for surface-enhanced optical phenomena such as Raman scattering, second harmonic generation, fluorescence, etc. [2-4]. SPPs and localized plasmons at dielectric-metal interfaces open up a previously inaccessible length scale for optical research. The intrinsically two-dimensional nature of SPPs provides great flexibility in engineering photonic circuits with submicron dimensions needed for optical communications and optical computing [5-7]. It would be greatly advantageous to take concepts such as highly localized waveguiding and surface-enhanced nonlinear effects to the terahertz (THz) regime, where a large variety of materials show specific resonances. At THz frequencies, however, metals resemble a perfect electric conductor (PEC), as their plasma frequencies are often in the ultraviolet part of the spectrum, leading to SPPs highly delocalized on metal surfaces [8, 9]. Recently, an idea of engineering surface plasmon at lower frequency was proposed [10]. That is, by cutting holes or grooves in metal surfaces to increase the penetration of EM fields into the metal, the frequency of existing surface plasmons can be tailored at will [11-13]. The existence of such geometry-controlled SPPs, named *spoof* SPPs, has recently been verified experimentally in the microwave regime [14].

So far, however, the properties of spoof SPPs at THz frequencies on corrugated metal surfaces have not yet been studied in detail, including the loss level of these spoof SPPs. In the previous theoretical studies of spoof SPPs, metals were all approximated by a perfect conductor, so that the spoof SPPs are lossless as they propagates along structured surfaces [10, 11]. The study of the characteristic of spoof SPPs at THz frequencies is of interest both for basic physics and for possible applications in device design. In this paper, we will study the properties of spoof SPPs at THz frequencies on aluminum (Al) surfaces corrugated periodically with grooves. For this purpose, a rigorous method for analyzing these spoof SPPs is formulated based on a modal expansion of EM fields. The finite conductivity of the metal as well as high-order modes within the grooves are taken into account in this formulation.

2. Method

Consider a metal surface in which a one-dimensional (1D) array of grooves of width a, depth h, and lattice constant d is drilled, as illustrated in the inset of Fig. 1(b). We are interested in H-polarized surface waves propagating in the x direction along the surface. The fields of these waves have the form of $\mathbf{H} = \hat{y}H_y$ and $\mathbf{E} = \hat{x}E_x + \hat{z}E_z$. Based on a modal expansion of the fields, H_y in region I ($z > 0$) can be written as

#86098 - $15.00 USD Received 6 Aug 2007; revised 24 Sep 2007; accepted 24 Sep 2007; published 27 Feb 2008

$$H_y^{\mathrm{I}}(x,z) = \sum_n A_n^{(1)} e^{-q_n^{(1)} z} e^{i\beta_n x}, \tag{1}$$

where $A_n^{(1)}$ are constants, $\beta_n = \beta + 2\pi n/d$ (here the propagation constant of the surface wave β lies in the first Brillouin zone, i.e., $|\mathrm{Re}(\beta)| \le \pi/d$, where $\mathrm{Re}(\cdot)$ denotes real part operator), and $q_n^{(1)} = \sqrt{(\beta_n)^2 - k_0^2}$ with k_0 being the wave number in free space. In region III ($z < -h$), H_y is similarly written as

$$H_y^{\mathrm{III}}(x,z) = \sum_n A_n^{(3)} e^{q_n^{(3)}(z+h)} e^{i\beta_n x}, \tag{2}$$

where $A_n^{(3)}$ are constants, $q_n^{(3)} = \sqrt{(\beta_n)^2 - \varepsilon_m k_0^2}$, and ε_m is the relative permittivity of the metal. On the other hand, since the metal thickness between the grooves ($d-a$) is much larger than the skin depth for THz frequencies, the fields in the part of the unit cell in region II ($-h \le z \le 0$) can be treated as a superposition of eigenmodes in an isolated groove waveguide. Thus, H_y in this part of the unit cell is expressed as

$$H_y^{\mathrm{II}}(x,z) = \sum_m \left[A_m^{(2)} e^{g_m(z+h/2)} + B_m^{(2)} e^{-g_m(z+h/2)} \right] \psi_m(x), \tag{3}$$

where $A_m^{(2)}$ and $B_m^{(2)}$ are constants, and the modal field profiles ψ_m are given by [15]

$$\psi_m(x) = \begin{cases} f(p_m a/2)\, \mathrm{e}^{-\gamma_m(x-a/2)}, & x > a/2 \\ f(p_m x), & |x| \le a/2 \\ f(-p_m a/2)\, \mathrm{e}^{\gamma_m(x+a/2)}, & x < -a/2 \end{cases}$$

where $p_m = \sqrt{k_0^2 - g_m^2}$, $\gamma_m = \sqrt{g_m^2 - \varepsilon_m k_0^2}$, and the function $f(\xi) = \cos(\xi)$ for symmetric modes with even m ($m = 0, 2, ...$), or $f(\xi) = \sin(\xi)$ for asymmetric modes with odd m ($m = 1, 3, ...$). Here, g_m and p_m are governed by the dispersion relation [15]: $\tan(p_m a/2) = \gamma_m/(\varepsilon_m p_m)$ for even m, or $\tan(p_m a/2 - \pi/2) = \gamma_m/(\varepsilon_m p_m)$ for odd m. Note that ψ_m have the property of orthogonality [15]

$$\frac{1}{a}\int_{-d/2}^{d/2} \frac{1}{\varepsilon(x)} \psi_m \psi_n dx \approx \frac{1}{a}\int_{-\infty}^{\infty} \frac{1}{\varepsilon(x)} \psi_m \psi_n dx = N_m \delta_{mn}, \tag{4}$$

where $\varepsilon(x) = 1$ for $|x| \le a/2$ and $\varepsilon(x) = \varepsilon_m$ elsewhere. N_m are coefficients depending on m.

The nonzero components (E_x and E_z) of the electric field (**E**) can be obtained straightforwardly from H_y. The parallel components of **E** and **H** must be continuous at the interface between regions I and II and the one between regions II and III. Matching boundary conditions at the interface $z = 0$, we obtain

$$A_m^{(2)} e^{ig_m h/2} - B_m^{(2)} e^{-ig_m h/2} = -i\frac{k_0}{q_0^{(1)}} \sum_{m'} U_{mm'} \left[A_{m'}^{(2)} e^{ig_{m'} h/2} + B_{m'}^{(2)} e^{-ig_{m'} h/2} \right], \tag{5}$$

where $U_{mm'}$ are given by

$$U_{mm'} = \frac{a}{dN_m} \frac{g_{m'}}{k_0} \sum_n \frac{q_0^{(1)}}{q_n^{(1)}} S_{mn}^{+} S_{m'n}^{-},$$

#86098 - $15.00 USD Received 6 Aug 2007; revised 24 Sep 2007; accepted 24 Sep 2007; published 27 Feb 2008

with

$$S_{mn}^{\pm} = \frac{1}{a}\int_{-d/2}^{d/2} \frac{1}{\varepsilon(x)}\psi_m(x)\exp(\pm i\beta_n x)dx,$$

where the coefficients N_m are defined in Eq. (4). Similarly, matching boundary conditions at the interface $z=-h$, we obtain

$$A_m^{(2)}e^{-ig_m h/2} - B_m^{(2)}e^{ig_m h/2} = -i\sqrt{-\varepsilon_m}\sum_{m'} V_{mm'}\left[A_{m'}^{(2)}e^{-ig_{m'}h/2} + B_{m'}^{(2)}e^{ig_{m'}h/2}\right], \tag{6}$$

where $V_{mm'}$ are given by

$$V_{mm'} = \frac{a}{dN_m}\frac{g_{m'}}{k_0}\sum_n S_{mn}^{+}S_{m'n}^{-}.$$

Note that $q_n^{(3)} \approx \sqrt{-\varepsilon_m}k_0$ since $|\varepsilon_m|$ is very large for THz frequencies. In the case of our interest, the groove width is much less than the wavelength (λ) of the surface wave, so all higher-order modes ($m \geq 1$) in the groove waveguide are evanescent, and their propagation constants g_m have a large imaginary part, i.e., $\mathrm{Im}(g_m) \approx m\pi/a$ (here $\mathrm{Im}(\cdot)$ denotes imaginary part operator), which results in very large values of $\exp(-ig_m h/2)$ in Eqs. (5) and (6) when the grooves are deep. To circumvent this numerical difficulty, we let $\zeta_m = \left(A_m^{(2)} - B_m^{(2)}\right)\sin(g_m h/2)$ and $\eta_m = \left(A_m^{(2)} + B_m^{(2)}\right)\cos(g_m h/2)$, and rewrite Eqs. (5) and (6) as

$$\zeta_m \cot(g_m h/2) + i\eta_m \tan(g_m h/2) = \frac{k_0}{q_0^{(1)}}\sum_{m'} U_{mm'}(\zeta_{m'} - i\eta_{m'}), \tag{7}$$

$$\zeta_m \cot(g_m h/2) - i\eta_m \tan(g_m h/2) = -\sqrt{-\varepsilon_m}\sum_{m'} V_{mm'}(\zeta_{m'} + i\eta_{m'}), \tag{8}$$

respectively, which can be expressed in a matrix form

$$K^{-1}[\zeta] + iK[\eta] = \frac{k_0}{q_0^{(1)}}U([\zeta] - i[\eta]), \tag{9}$$

$$K^{-1}[\zeta] - iK[\eta] = -\sqrt{-\varepsilon_m}V([\zeta] + i[\eta]), \tag{10}$$

where the vectors $[\zeta]$ and $[\eta]$ have a length equal to the number of modes included in Eq. (3). The diagonal matrix K is defined as $K_{mm'} = \tan(g_m h/2)\,\delta_{mm'}$, and K^{-1} is the inverse matrix of K. From Eq. (10), we have approximately

$$[\zeta] + i[\eta] = -\frac{1}{\sqrt{-\varepsilon_m}}V^{-1}\left(K + K^{-1}\right)[\zeta]. \tag{11}$$

Substitution of Eq. (11) into Eq. (9) yields the equation $\mathrm{Q}[\zeta] = \left(q_0^{(1)}/k_0\right)[\zeta]$ with

$$\mathrm{Q} = K_a^{-1}\left\{U + \frac{1}{\sqrt{-\varepsilon_m}}\left[U + \frac{q_0^{(1)}}{k_0}K\right]V^{-1}K_b\right\},$$

where $K_a = (K^{-1} - K)/2$ and $K_b = (K^{-1} + K)/2$. Evidently, K_a and K_b are a diagonal matrix, and we easily find that $\{K_a\}_{m,m} = \cot(g_m h)$ and $\{K_b\}_{m,m} = [1/\sin(g_m h)]$. Finally, we obtain the dispersion relation for spoof SPPs on the corrugated surface in the form

$$\det\left\{Q - \frac{q_0^{(1)}}{k_0}I\right\} = 0, \tag{12}$$

#86098 - $15.00 USD Received 6 Aug 2007; revised 24 Sep 2007; accepted 24 Sep 2007; published 27 Feb 2008

where I is a unit matrix. Note that $q_0^{(1)} = \sqrt{\beta^2 - k_0^2}$. Equation (12) can be solved numerically via iteration for $q_0^{(1)}$ or β. If the metal is a PEC, i.e., $|\varepsilon_m| \to \infty$, the matrix Q reduces to $Q = K_a^{-1}U$, and Eq. (12) becomes $\det\{K_a^{-1}U - (q_0^{(1)}/k_0)I\} = 0$. If we further neglect the effect of higher-order modes within grooves, i.e., only the lowest-order ($m = 0$) mode is included in the expansion, the dispersion equation is simplified to $q_0^{(1)} = (a/d)k_0 \tan(k_0 h)$ in the limit $\lambda \gg d$, which is identical to Eq. (9) of Ref. [11]. The solution of this dispersion equation offers an initial value of iteration for $q_0^{(1)}$ in solving Eq. (12).

3. Results

To validate the proposed dispersion relation for spoof SPPs on a corrugated metal surface, we first analyze its convergence for modal expansion. In what follows, the metal is assumed to be Al, and its dielectric properties are modelled by a Drude model with the parameters taken from Refs. [16, 17]. Here, as an example, the lattice constant is $d = 50$ μm, and the groove depth is $h = d$. Two groove widths are considered: (1) $a = 0.2d$, (2) $a = 0.6d$. The asymptotic frequencies for two cases, which are evaluated at $\mathrm{Re}(\beta) = \pi/d$ (i.e., the border of the first Brillouin zone), are $f_s = 1.275$ and 1.165 THz, respectively. The frequency of the surface wave is set to $f = 0.8$ THz. The calculated results are plotted in Fig. 1, where the corresponding results obtained within the PEC approximation are included as triangles for comparison. As seen from Fig. 1, both $\mathrm{Re}(\beta)$ and $\mathrm{Im}(\beta)$ converge rapidly. The results of $\mathrm{Re}(\beta)$ in the single-mode ($m = 0$) approximation are accurate within 3% for both cases. The difference between the values of $\mathrm{Re}(\beta)$ for Al and those for PEC are almost negligible, meaning that the model with the PEC approximation is valid for analyzing the dispersion of spoof SPPs at THz frequencies. The result of $\mathrm{Im}(\beta)$ obtained within the single-mode approximation is always larger than the accurate value (see Fig. 1(b)), and its relative error is 2.4% for the case with $a = 0.2d$ and nearly 10% for the case with $a = 0.6d$. Our analysis indicates that in the latter case, the relative error becomes 88.7% when $f = 1.15$ THz. Evidently, a few modes with higher orders become important when the groove width is large, especially at frequencies close to the asymptotic frequency of the surface structure.

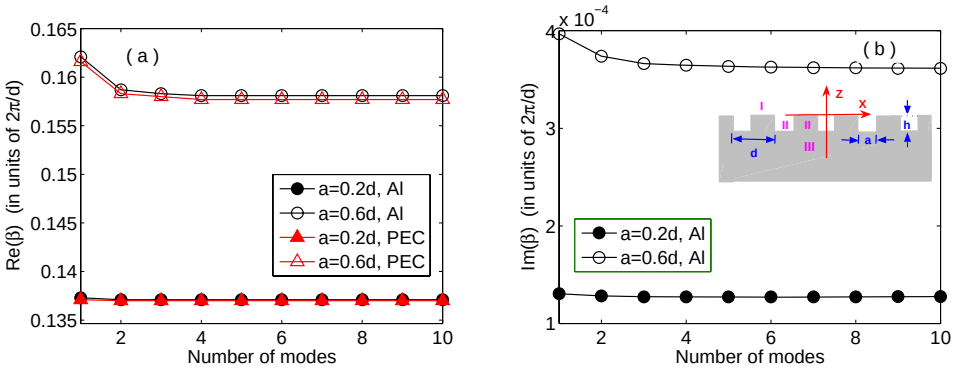

Fig. 1. Convergence of the real (a) and imaginary (b) parts of the propagation constant β calculated from Eq. (12) for $d = 50$ μm, $h = 50$ μm, and $f = 0.8$ THz. The corresponding results obtained within the PEC approximation are included as triangles for comparison. The inset shows the geometry of structured surface.

We now analyze the properties of spoof SPPs at THz frequencies on periodically corrugated Al surfaces. Figure 2(a) shows the dispersion curves for spoof SPPs on structured surfaces with

#86098 - $15.00 USD Received 6 Aug 2007; revised 24 Sep 2007; accepted 24 Sep 2007; published 27 Feb 2008

$d = 50$ μm. Two groove depths are analyzed: $h = d$ and $h = 0.5d$. For each groove depth, several values of the groove width are shown. As seen from Fig. 2(a), the larger the groove depth, the lower the asymptotic frequency. This is also the situation for the groove width. But compared with the groove depth, the groove width weakly affects the asymptotic frequency. Figure 2(b) shows the losses of these spoof SPPs as a function of frequency. The loss of spoof SPPs grows significantly with increasing frequency. For example, in the case of $a = 0.2d$ and $h = d$, the attenuation coefficient of the spoof SPPs is 0.045 cm^{-1} for $f = 0.6$ THz, and it becomes 0.16 cm^{-1} for $f = 0.8$ THz and 0.7 cm^{-1} for $f = 1$ THz. Compared to purely dielectric THz waveguides reported in Refs. [18, 19], the corrugated metal surface exhibits relatively high loss for guiding THz wave when the wave field is effectively confined. Evidently, the loss of the spoof SPPs increases when the confinement of the fields of the spoof SPPs is enhanced. The field is more strongly confined to the surface for a larger frequency. This is displayed in Fig. 3, where the distribution of the **H** field in a unit cell of the surface structure is plotted for various frequencies. As shown in Fig. 3, the field of the surface wave is almost concentrated in the structured surface when $f = 1$ and 1.2 THz. Figure 2(b) clearly shows that for a given frequency, a larger groove width or depth correspond to a larger loss of spoof SPPs. As a larger groove width or depth correspond to a lower asymptotic frequency, leading to a larger departure of the propagation constant for a given frequency from the light line (see Fig. 2(a)). Correspondingly, the z component of the wave vector $q_0^{(1)} = \sqrt{\beta^2 - k_0^2}$ becomes larger, thus increasing the field confinement and the loss of the SPPs.

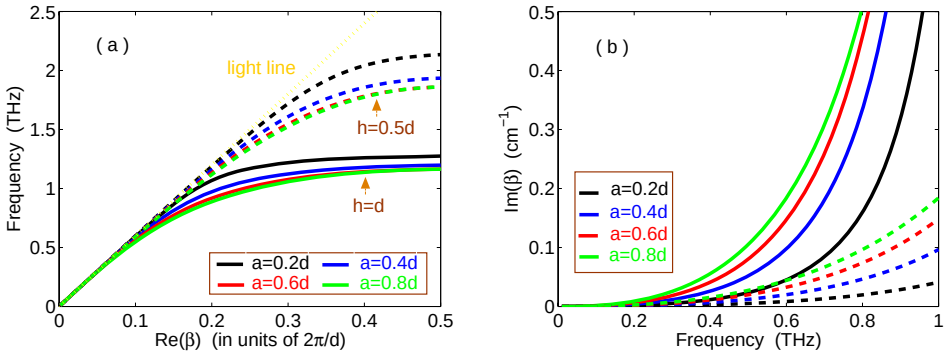

Fig. 2. (a) Dispersion curves for spoof SPPs. (b) Attenuation coefficients of spoof SPPs. The lattice constant is $d = 50$ μm. The solid and dashed lines correspond to the groove depths $h = d$ and $h = 0.5d$, respectively.

It is interesting to analyze the effect of the lattice constant (d) on the dispersion and loss of spoof SPPs. Figure 4(a) shows the dispersion curves for spoof SPPs on corrugated surfaces with different lattice constants $d = 35$, 50, and 75 μm. The groove parameters are $a = 10$ μm and $h = 50$ μm for all cases. The losses of spoof SPPs for three cases are plotted in Fig. 4(b). As seen from Figs. 4(a) and 4(b), a smaller lattice constant corresponds to a larger asymptotic frequency (indicated by dotted line in the Fig. 4(a)), but it corresponds to a larger loss of spoof SPPs for a given frequency. Evidently, a structured surface with a smaller lattice constant possesses a higher asymptotic frequency only because it allow spoof SPPs to have a larger range of propagation constant. But the asymptotic frequency doesn't seem to be sensitive to the lattice constant. However, as shown in Fig. 4(b), the loss of the spoof SPPs is quite sensitive to the lattice constant. For a given frequency, an increase of the lattice constant may lead to a considerable reduction in the loss of spoof SPPs.

#86098 - $15.00 USD Received 6 Aug 2007; revised 24 Sep 2007; accepted 24 Sep 2007; published 27 Feb 2008

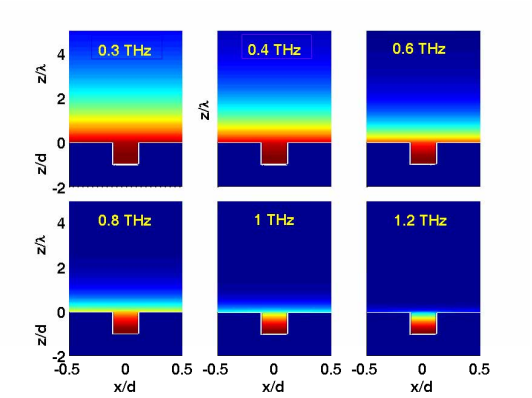

Fig. 3. Spatial variation of the amplitude of the **H** field in a unit cell of the surface structure with $d = 50$ μm, $a = 0.2d$, and $h = d$. For clarity, different length scales are used in the z direction for $z \leq 0$ and $z > 0$.

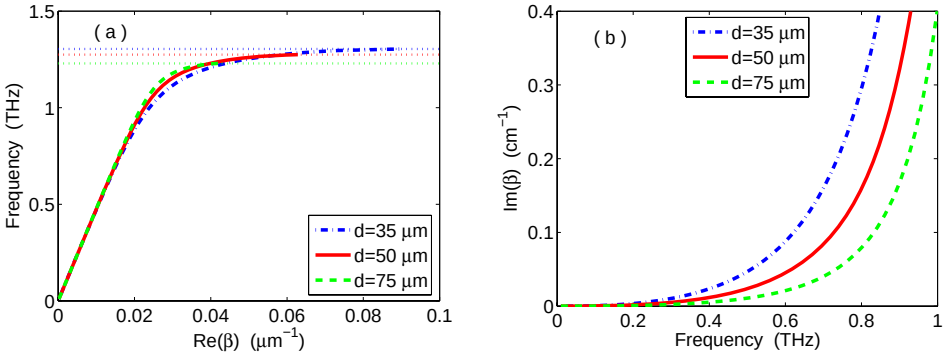

Fig. 4. Dispersion relations (a) and attenuation coefficients (b) of spoof SPPs for different lattice constants $d = 35$, 50, and 75 μm. The parameters of the groove geometry are $a = 10$ μm and $h = 50$ μm. Dotted lines indicate the asymptotic frequencies for three cases.

For spoof SPPs at THz frequencies, the property of the strong confinement of the fields contradicts with that of low propagation loss. However, there exists possibility of optimum design for spoof SPPs to relieve this contradiction. To illustrate this, we analyze the field confinement of spoof SPPs for different groove cases under the condition that the loss of the related SPPs is kept at a constant low level. The field confinement of spoof SPPs in free space can be characterized by the parameter $D = 1/q_0^{(1)}$, where $q_0^{(1)} = \sqrt{\beta^2 - k_0^2}$. As an example, the lattice constant is $d = 50$ μm, and the frequency is $f = 0.6$ THz. The constant loss for spoof SPPs is set to $\mathrm{Im}(\beta) = 0.045$ cm^{-1}, which corresponds to the value for the case of $a = 0.2d$ and $h = d$. The calculated results are plotted in Fig. 5. Figure 5(a) shows the groove depth as a function of the groove width. Note that for each pair of a and d in Fig. 5(a), the attenuation coefficient of spoof SPPs at $f = 0.6$ THz is always equal to 0.045 cm^{-1}. The values of D for different sets of groove parameters are shown in Fig. 5(b), and a minimum of $D = 0.8\lambda$ occurs at $a = 0.6d$, where the corresponding groove depth is $h = 0.6d$. Figures 5(c) and 5(d) show the distribution of the **H** field in the unit cell for $a = 0.2d$ ($h = d$ correspondingly) and $a = 0.6d$ ($h = 0.6d$), and the improvement of field confinement in the latter case is clearly observed. Our analysis indicates

#86098 - $15.00 USD Received 6 Aug 2007; revised 24 Sep 2007; accepted 24 Sep 2007; published 27 Feb 2008

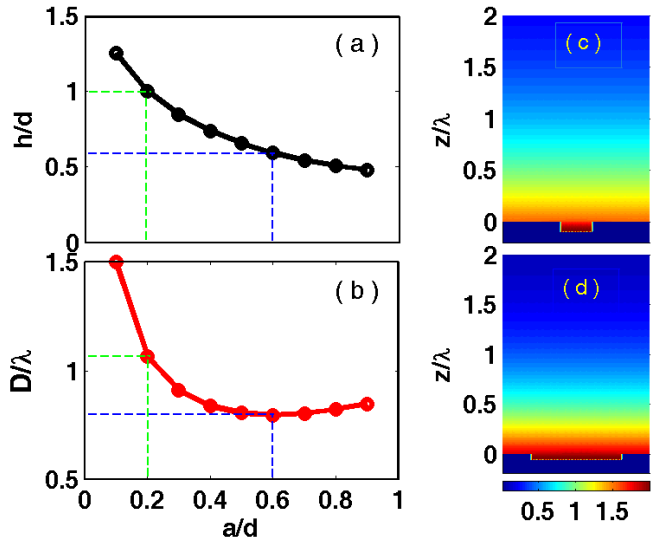

Fig. 5. (a) Groove depth versus the groove width. (b) Parameter D versus the groove width for $f = 0.6$ THz. Note that for each groove case in (a), the attenuation coefficient of spoof SPPs at $f = 0.6$ THz is always equal to $\mathrm{Im}(\beta) = 0.045$ cm^{-1}. (c)-(d) Spatial variation of the amplitude of the **H** field at $f = 0.6$ THz for the cases with $a = 0.2d$ ($h = d$) and $a = 0.6d$ ($h = 0.6d$), respectively. The lattice constant is $d = 50$ μm.

that in the optimum case the **H** field is concentrated in a region of 0.7λ on the structure surface. As the field components with higher spatial frequencies β_n ($n \neq 0$) in Eq. (1) are more strongly confined to the surface than the one with β (i.e., $n = 0$), which is dominant in general, the total field in free space is actually confined over a distance less than D.

4. Conclusion

A rigorous method for analyzing spoof SPPs on a periodically corrugated metal surface has been formulated based on a modal expansion of electromagnetic fields. Compared to the previous method, our method is able to calculate the loss of these spoof SPPs, since it takes into account the finite conductivity of the metal. Also, higher-order modes within the grooves of the surface structure are included in our method. The convergence analysis shows that a few modes with higher orders are not negligible when the groove width is relatively large, especially at frequencies close to the asymptotic frequency. In the THz frequency range, the properties of the dispersion and loss of spoof SPPs on corrugated Al surfaces have been analyzed. The asymptotic frequency of spoof SPPs mainly depends on the groove depth, but the loss of spoof SPPs is sensitive to all the parameters of surface structure, including the lattice constant. The loss of the spoof SPPs grows significantly as the field confinement is enhanced, and the loss is often considerably large at frequencies close to the asymptotic frequency. But the performance of both low-loss propagation and subwavelength field confinement for spoof SPPs can be achieved by the optimum design of surface structure.

Acknowledgements

This work was supported by the Ministry of Education (Singapore) under Grant No. R263000357112 and R263000357133.

#86098 - $15.00 USD Received 6 Aug 2007; revised 24 Sep 2007; accepted 24 Sep 2007; published 27 Feb 2008